



Effect of Porcine *Clostridium perfringens* on Intestinal Barrier, Immunity, and Quantitative Analysis of Intestinal Bacterial Communities in Mice

Zipeng Jiang^{1,2,3,4,5}, Weifa Su^{1,2,3,4,5}, Chaoyue Wen^{1,2,3,4,5}, Wentao Li^{1,2,3,4,5}, Yu Zhang^{1,2,3,4,5}, Tao Gong^{1,2,3,4,5}, Shuai Du^{1,2,3,4,5}, Xinxia Wang^{1,2,3,4,5}, Zeqing Lu^{1,2,3,4,5*}, Mingliang Jin^{1,2,3,4,5} and Yizhen Wang^{1,2,3,4,5*}

¹ National Engineering Laboratory of Biological Feed Safety and Pollution Prevention and Control, Zhejiang University, Hangzhou, China, ² Key Laboratory of Molecular Nutrition, Ministry of Education, Zhejiang University, Hangzhou, China, ³ Key Laboratory of Animal Nutrition and Feed, Ministry of Agriculture and Rural Affairs, Zhejiang University, Hangzhou, China, ⁴ Key Laboratory of Animal Nutrition and Feed Nutrition of Zhejiang Province, Zhejiang University, Hangzhou, China, ⁵ College of Animal Science, Institute of Feed Science, Zhejiang University, Hangzhou, China

OPEN ACCESS

Edited by:

Peck Toung Ooi,
Putra Malaysia University, Malaysia

Reviewed by:

Yanping Wu,
Zhejiang Agriculture and Forestry
University, China
Yichao Yang,
Yale University, United States

*Correspondence:

Zeqing Lu
zqlu2012@zju.edu.cn
Yizhen Wang
yzwang321@zju.edu.cn

Specialty section:

This article was submitted to
Veterinary Infectious Diseases,
a section of the journal
Frontiers in Veterinary Science

Received: 23 February 2022

Accepted: 26 April 2022

Published: 13 June 2022

Citation:

Jiang Z, Su W, Wen C, Li W, Zhang Y,
Gong T, Du S, Wang X, Lu Z, Jin M
and Wang Y (2022) Effect of Porcine
Clostridium perfringens on Intestinal
Barrier, Immunity, and Quantitative
Analysis of Intestinal Bacterial
Communities in Mice.
Front. Vet. Sci. 9:881878.
doi: 10.3389/fvets.2022.881878

Clostridium perfringens (*C. perfringens*) is one of the main pathogens which can cause a range of histotoxic and enteric diseases in humans or animals (pigs, or broilers). The Centers for Disease Control and Prevention (CDC) estimates these bacteria cause nearly 1 million illnesses in the United States every year. For animal husbandry, necrotizing enteritis caused by *C. perfringens* can cost the global livestock industry between \$2 billion and \$6 billion per year. *C. perfringens*-infected animals can be isolated for its identification and pathology. A suitable animal model is one of the essential conditions for studying the disease pathogenesis. In previous studies, mice have been used as subjects for a variety of *Clostridium perfringens* toxicity tests. Thus, this study was designed to build a mouse model infected porcine *C. perfringens* which was isolated from the *C. perfringens*-infected pigs. A total of 32 6-week-old male C57BL/6 mice were randomly divided into four groups. Control group was orally administrated with PBS (200 μ L) on day 0. Low group, Medium group, and High group were gavaged with 200 μ L of PBS resuspension containing 8.0×10^7 CFU, 4.0×10^8 CFU, and 2.0×10^9 CFU, respectively. We examined growth performance, immune status, intestinal barrier integrity, apoptosis-related genes expression, and copies of *C. perfringens* in mice. The results showed that the growth performance declined and intestinal structure was seriously damaged in High group. Meanwhile, pro-inflammatory factors (IL-1 β , TNF- α , and IL-6) were significantly increased ($P < 0.05$) in High group compared to other groups. The tight junctions and pro-apoptosis related genes' expression significantly decreased ($P < 0.05$) in High group, and high dose caused a disruption of intestinal villi integrity and tissue injury in the jejunum of mice. In addition, the enumerations of *C. perfringens*, *Escherichia coli*, and *Lactobacillus* explained why the gut of High group mice was seriously damaged, because the *C. perfringens* and *Escherichia coli* significantly

enriched ($P < 0.05$), and *Lactobacillus* dramatically decreased ($P < 0.05$). Overall, our results provide an experimental and theoretical basis for understanding the pathogenesis and exploring the effects of porcine *C. perfringens* on mice.

Keywords: *Clostridium perfringens*, mice model, intestinal barrier, immune status, apoptosis

INTRODUCTION

Clostridium perfringens is a gram-positive, spore-forming, anaerobic, rod-shaped bacterium (1). *C. perfringens* was isolated from a broad range of environments, such as the soil, freshwater sediment, and the gastrointestinal track of human and animals (2). As an opportunistic pathogen [opportunistic pathogen is one that generally does not harm its host but can when the host's resistance is low (3)], *C. perfringens* can cause disease; it causes a range of histotoxic and enteric diseases in humans and animals (4). *C. perfringens* bacteria are one of the most common causes of foodborne illness (food poisoning). The Centers for Disease Control and Prevention (CDC) estimates these bacteria cause nearly 1 million illnesses in the United States every year (5, 6). For animal husbandry, necrotizing enteritis caused by *C. perfringens* can cost the global livestock industry between \$2 billion and \$6 billion per year (7, 8). *C. perfringens* mainly causes hemorrhagic necrotizing enteritis in piglets, and triggers "sudden death" disease characterized by abdominal bulging in fattening pigs and pregnant sows, with an 100% mortality rate (9). It is necessary to fully explore the prevention and treatment methods for the disease caused by *C. perfringens* in pigs. Therefore, establishing an animal model is the best way to visually study and obtain data on pathological damage.

A suitable animal model is one of the essential conditions for studying the disease pathogenesis (10). Some studies have used intramuscular or intravenous injections to establish mouse models of *C. perfringens* infection (11–13), and others have modeled *D. aeruginosa* by inoculation in the duodenum, intragastric inoculation, or by imposing an oral challenge (14–17). These studies focused on results primarily from a toxemia following absorption of toxins from the intestine into the circulation and they did not fully investigate the concrete changes during *C. perfringens* infection. In the present study, we use the mouse model for understanding the pathogenesis of porcine *C. perfringens* by oral gavage. Furthermore, negative effects (weight loss, decreased expression of tight junction proteins, intestinal morphological damage, etc.) of porcine *C. perfringens* in mouse model were evaluated by determining intestinal morphology, immune status, intestinal barriers integrity, apoptosis, and enumerations of pathogens or probiotics. Our study aims to provide a suitable animal model for the research of the prevention of a pathogenic mechanism of porcine *C. perfringens*.

MATERIALS AND METHODS

All the procedures were approved by the Institutional Animal Care and Use Committee at Zhejiang University.

Bacterial Strain Preparation

Our laboratory originally isolated the pathogenic bacterium which induced the death of swine in a farm from Tech-Bank Co., Ltd. This bacterium was extracted by bacteria genomic DNA kit (Tiangen Biotech Co., Ltd. Beijing). Then PCR amplification was performed using 16S rDNA specific primers and PCR products were subject to purification and Sanger sequencing. We exerted the NCBI (Gene Bank database) to detect the species of this pathogen. In this experiment, this porcine *C. perfringens* was cultured anaerobically on tryptose-sulfite-cycloserine (TSC) agar for 18 h at 37°C, and then transferred to a reinforced clostridium medium (RCM) for analysis (anaerobic environment). The bacteria were harvested by centrifugation at 4,000 g for 10 min at 4°C, and washed 3 times with phosphate-buffered saline (PBS) solution. Finally, we obtained 8.0×10^7 to 2.0×10^9 CFU (colony forming units) *C. perfringens*.

Animals Experiment

Thirty-two mice (5-week-old male C57BL/6) were purchased from Shanghai Laboratory Animal Co., Ltd. (SLAC, Shanghai, China). All mice were randomly divided into four groups (Figure 1) after 1-week adaptation: Control group, Low group, Medium group, and High group. Mice in Control group were treated orally with 200 μ l PBS. Meanwhile, mice in the Low, Medium, and High groups were gavaged with 200 μ l of PBS resuspension containing 8.0×10^7 CFU, 4.0×10^8 CFU, and 2.0×10^9 CFU, respectively. Mice were weighed every single day and offered free access to the water and feed during the experimental period. The animal experimental protocol was approved by the Animal Care and Use Committee of Zhejiang University.

Sample Collection

On day 7, all mice in each group were weighed and sacrificed to collect liver, spleen, colon, blood samples, jejunum, ileum, and fresh digesta in the intestine. The weight of liver and spleen were recorded and was used to calculate the organ index. The colon length was measured by vernier caliper. The blood samples were collected by cardiac puncture and centrifugated at 3,000 g for 10 min at 4°C, then serum was obtained. The jejunum was washed with cold PBS and prepared for morphology analysis and gene expression determination (–80°C). Simultaneously, the digesta in the intestine were obtained for determining the microbiota enumeration.

Intestinal Morphology Analysis

The tissues of duodenum, jejunum, and ileum were fixed by 4% paraformaldehyde, then these tissues were excised, embedded in paraffin, sliced, and stained with hematoxylin an eosin (H&E) according to pervious methods (18, 19). Images of paraffin section were observed and obtained with a Lecia DM3000

Microsystem (Leica, Wetzlar, Germany). The villus height and crypt depth were measured by previous studies (19, 20). All paraffin sections were determined from at least 10 well-oriented villus-crypt units by upright fluorescence microscopy using a BX51 microscope (Olympus, Tokyo, Japan).

Inflammatory Cytokines and Immunoglobulin in Serum and Feces of Mice

Serum parameters, including inflammatory cytokines IL-1 β , IL-6, TNF- α and immunoglobulin IgA, IgG, and fecal sIgA, were determined using ELISA kits (Jiangsu Enzyme-Labeled Biological Technology, Jiangsu, China). The protocols were carried out according to the manufacturer's instructions and followed by previous studies (21). Standard 50 μ l was added to standard well, then 40 μ l sample dilution was added to the testing sample well, then 10 μ l testing sample was added (sample final dilution is 5-fold). To each well, 100 μ l HRP-conjugate reagent was added. After closing plate with the closure plate membrane, the samples were incubated for 60 min at 37°C. After uncovering the late membrane, the liquid was discarded, dried by swinging, and washing buffer was added to every well, kept still for 30s and then drained. This was repeated 5 times and then the membranes were pat dry. Chromogen Solution A 50 μ l and Chromogen Solution B were added to each well, with light preservation evaded for

15 min at 37°C. Stop Solution of 50 μ l was added to each well. The reaction was then stopped (the blue color changed to yellow color). The blank well was taken as zero, and absorbance was read at 450 nm after adding Stop Solution and within 15 min.

RNA Extraction and Gene Expression Analysis

Total RNA isolation from the tissues was carried out according to previous studies (22, 23), using Trizol reagent (Invitrogen Life Technologies, Carlsbad, CA) according to the manufacturer's instructions. NanoDrop 2000 (Thermo Scientific, Waltham, MA,

TABLE 2 | The sequence of 16s rRNA qRT-PCR primers used to quantify intestinal bacteria.

| Target | Primer sequence (5'-3') | Amplicon size, bp | Reference |
|--------------------------------|---------------------------|-------------------|-----------|
| <i>Clostridium perfringens</i> | F: ATGCAAGTCGAGCGAKG | 105 | (27) |
| | R: TATGCGGTATTAATCTYCCTTT | | |
| <i>Lactobacillus subgroup</i> | F: AGCAGTAGGGAATCTTCCA | 341 | (25) |
| | R: CACCGCTACACATGGAG | | |
| <i>Escherichia subgroup</i> | F: GTTAATACCTTGCTCATTGA | 340 | (24) |
| | R: ACCAGGGTATCTAATCCTGT | | |

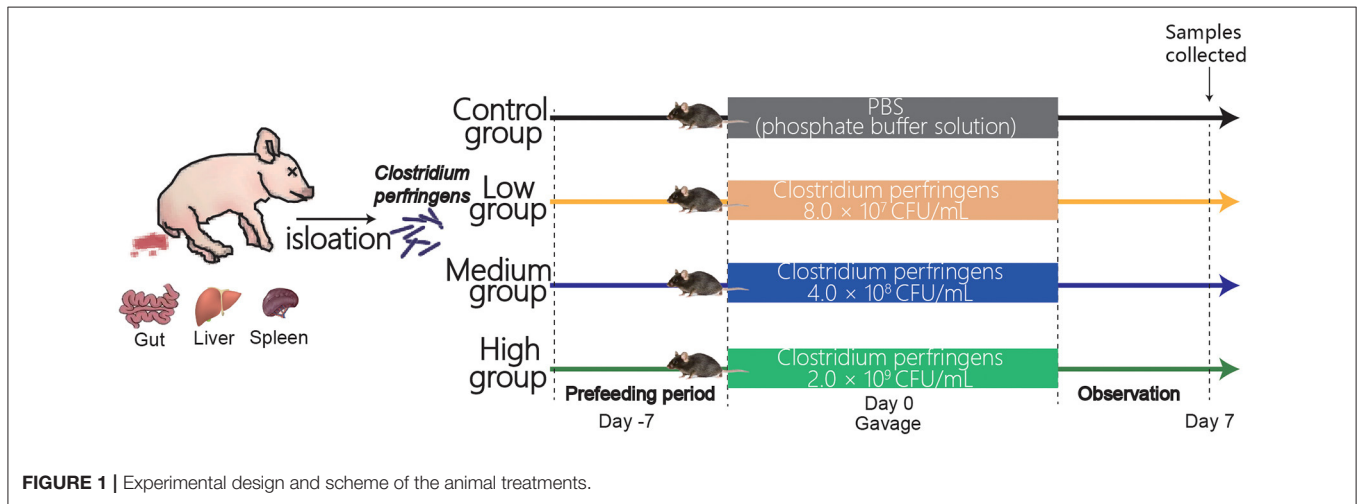


FIGURE 1 | Experimental design and scheme of the animal treatments.

TABLE 1 | Primer sequences for q-PCR.

| Gene | Forward primer sequence (5' –3') | Reverse primer sequence (5' –3') | Accession number |
|----------------|----------------------------------|----------------------------------|------------------|
| β -actin | CTAGGCGGACTGTTACTGAGC | CGCCTTCACCGTTCCAGTTT | NM_007393.5 |
| ZO-1 | GAAGTTACGTGCGGGAGCAG | GGGACAAAAGTCCGGGAAGC | NM_001163574.1 |
| MUC-2 | GCCACCTCACAAGCAGTAT | GTCATAGCCAGGGGCAAAC | NM_023566.4 |
| Claudin1 | TATGACCCCTTGACCCCAT | AGAGGTTGTTTTCCGGGGAC | NM_016674.4 |
| Occludin | TGAGCACCTTGGGATTCCG | AAAAGGCCTCACGGACATGG | NM_008756.2 |
| p53 | GGGCTGAGACACAATCCTCC | CATTGTAGGTGCCAGGGTCC | NM_001127233.1 |
| Bax | CTGGATCCAAGACCAGGGTG | CCTTTCCCTTCCCCATTC | NM_009527.3 |
| BCL-2 | TGAGTACCTGAACCGGCATC | TTGTGGCCAGGTATGCAC | NM_009741.5 |
| Caspase-3 | GCTTGGAACGGTACGCTAAG | CCACTGACTTGCTCCCATGT | NM_001284409.1 |
| Caspase-9 | CACCTTCCCAGGTTGCCAAT | CAAGCCATGAGAGCTTCGGA | NM_001277932.1 |

USA) was used to measure the optical density at 260 to 280 and quantified the purity of the RNA. One microgram of total RNA was reverse transcribed by the reverse transcription kit (Takara Biotechnology Inc., Ostu, Japan) with random primers following the manufacturer's instructions. Subsequently, all the cDNA were obtained. The mRNA expression of *zonula occludens 1 (ZO-1)*, *Occludin*, *Claudin1*, *MUC2*, *p53*, *Bax*, *Bcl-2*, *Caspase-3*, and *Caspase-9* in the jejunum were measured by quantitative real-time PCR (qRT-PCR) analysis. The qRT-PCR assay was conducted on a StepOne Real-Time PCR System (ABI StepOnePlus, Applied Biosystem, Foster City, California) using commercial SYBR-Green PCR-kit (Takara Biotechnology Inc., Japan). Gene-specific primers (Table 1) were used for this process. Finally, the β -actin was used as the housekeeping gene, and relative mRNA gene expression were detected by using the $2^{-\Delta\Delta C_t}$ method as previously described (21).

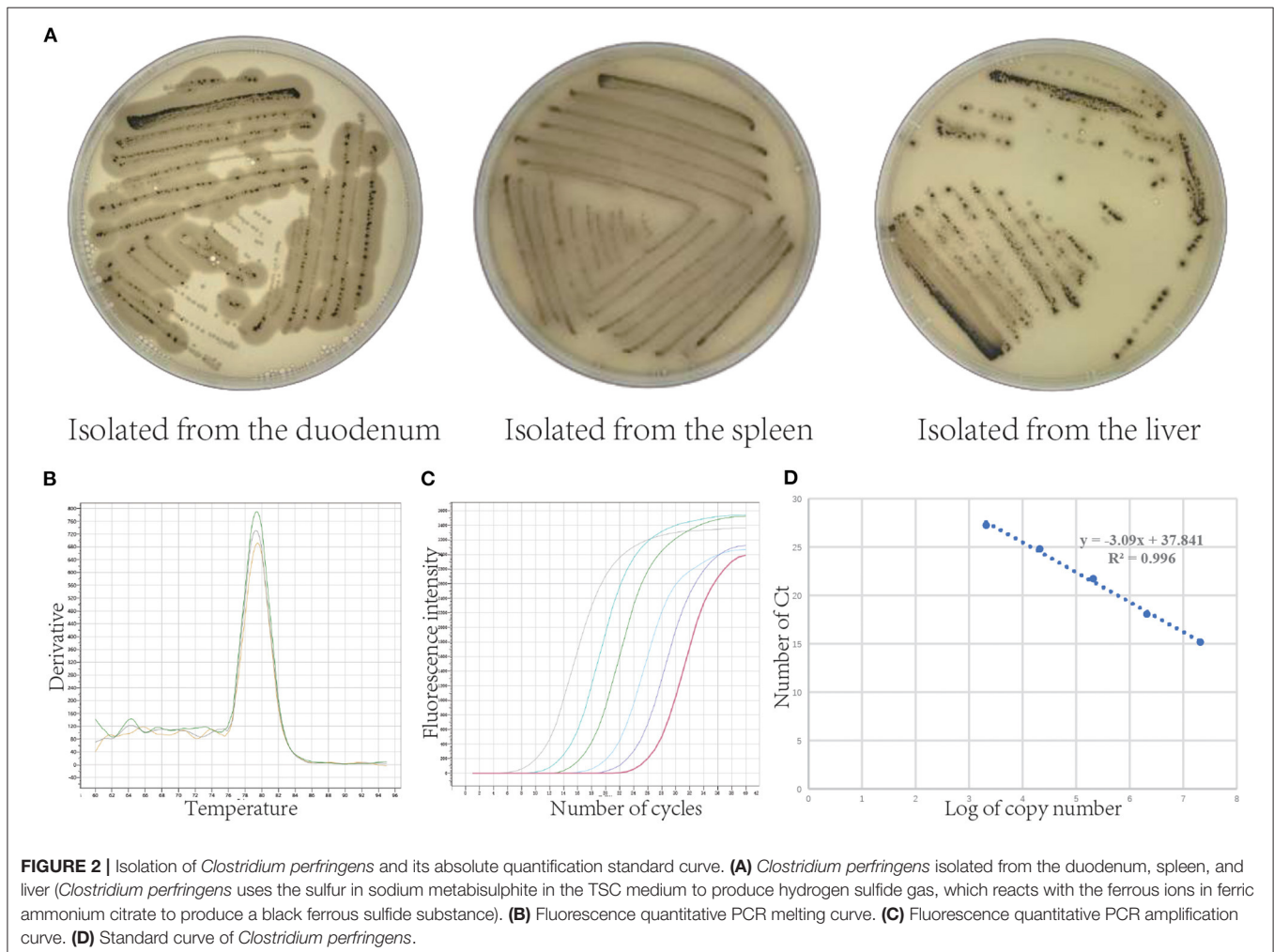
(24–26). The QIAamp DNA Mini Kit (QIAGENLtd., Hilden, Germany) was exerted to isolate the genomic DNA from the ileum and caecum (200 mg of digesta). Extracted DNA was stored at -80°C for further analysis.

Normal PCR amplification was used to produce high concentrations of the target DNA from pure bacterial cultures and standard curves were prepared using it. Primer sequences were designed on the basis of 16s rRNA according to the previous study (Table 2) (28). Competent *Escherichia coli* DH5 α (Takara Bio Inc., Japan) was applied to generate plasmid standards. PCR purification kit (Biomed Gene Technologies, Beijing, China) was used to purify PCR products and TA cloning kit (Invitrogen Corporation, Carlsbad, CA, USA) was accessed to clone into pCRTM2.1 as per the manufacturer's instruction. Nanodrop 2000 (Thermo Fisher Scientific Inc., Waltham, MA, USA) was exerted to quantify the purified insert-containing plasmids. Then the number of target DNA copies was calculated by the following formula according to Lee et al. (29).

***Clostridium perfringens* Enumeration of Ileum and Cecum**

The population of *C. perfringens* in the digesta was detected by absolute qRT-PCR methods, described in previous studies

$$\text{DNA (copy)} = \frac{6.02 \times 10^{23} \text{ (copy/mol)} \times \text{DNA amount (g)}}{\text{DNA length (dp)} \times 660 \text{ (g/mol/dp)}}$$



Ten-fold serial dilutions of plasmid DNA method were supported to construct the Standard curve. Finally, the DNA from ileal and cecal samples was determined for absolute qRT-PCR using a StepOne Real-Time PCR System (ABI StepOnePlus, Applied Biosystem, Foster City, California) according to commercial SYBR-Green PCR-kit (Takara Biotechnology Inc., Japan) protocols.

Statistical Analysis

SPSS 20.0 software (SAS Inc., Chicago, IL) was used for analyzing the present study data. One-way ANOVA and Duncan's test were used to determine the difference among groups. Data were expressed as the mean \pm standard deviation (SD). $P < 0.05$ was considered statistically significant. GraphPad Prism 8 (San Diego, CA, USA) was used to generate bar plots.

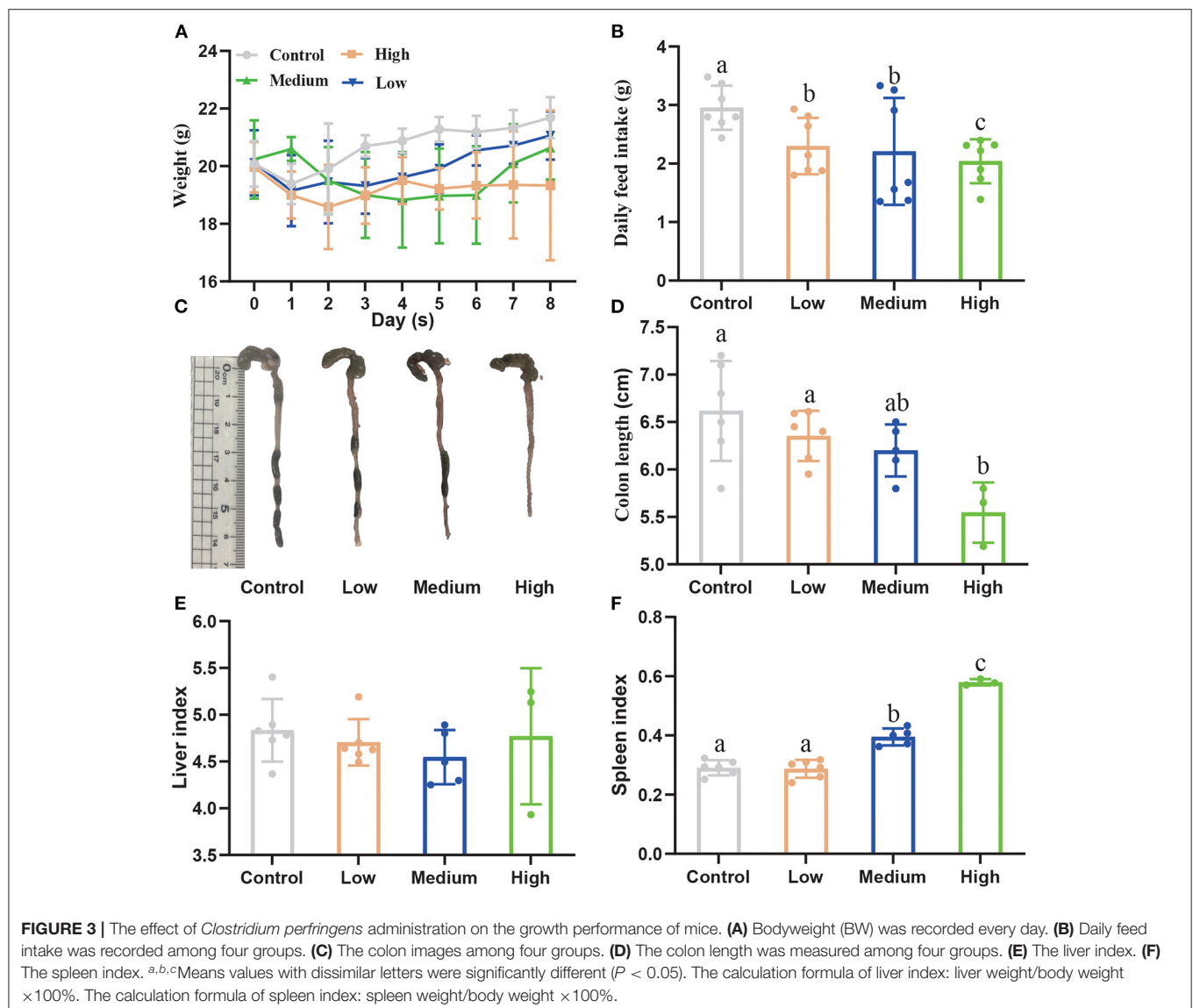
RESULTS

Isolation of *Clostridium perfringens* and Construction of Standard Curve

As shown in **Figure 2A**, *C. perfringens* was separated from the duodenum, spleen, and liver of pigs (flatulence death). We determined that the pathogen is *C. perfringens* (Gene Bank: OL454188) which was 99.79 % identical with *C. perfringens* ATCC13124. **Figures 2B,C** showed the melting curve and the amplification curve of fluorescence quantitative PCR, which indicated that the process of qRT-PCR is correct. **Figure 2D** is the standard curve of absolute quantification ($y = -3.09x + 37.841$, $R^2 = 0.996$). The standard curve was used to calculate the copies/g of *C. perfringens* concentration.

Growth Performance and Mortality of Mice

Figure 3A showed the body weights (BW) among four groups during the experimental period. After being challenged with



porcine *C. perfringens*, the BW of High group and Medium group decreased from day 1 and 2. Then the BW increased from day 5 to 8 in Medium group, while the BW of High group declined continuously compared with Control group. On day 8, the BW of High group (19.34 ± 1.06 g) significantly decreased ($P < 0.05$) compared with Control group (21.68 ± 0.29 g), whereas Medium group (20.64 ± 0.45 g) and Low group (21.07 ± 0.34 g) had no significant difference ($P > 0.05$) with Control group. Meanwhile, the daily feed intake of all *C. perfringens* treatment groups presented a significant decline ($P < 0.05$) compared with Control group (Figure 3B). Figures 3C,D showed that the colon length dramatically reduced ($P < 0.05$) after high dose treatment, compared with Control group. The liver index (Figure 3E) showed no significant difference ($P > 0.05$) among four groups, while the spleen index (Figure 3F) increased notably ($P < 0.05$) in High and Medium group in contrast to Control group.

After gavage, all groups except Control group displayed the clinical symptoms (Table 3) and the mortality was 12.5% (Low group), 37.5% (Medium group), and 50% (High group), respectively. As the dose rose, Figure 4 showed that the time of death appeared early and the death number further increased.

Clostridium perfringens Stimulated the Injury of Intestines

Compared to the Control group, the High group exhibited extremely discontinuous brush edges and blunt villus in duodenum, jejunum, and ileum, while Low group had a litter influence which was induced by *C. perfringens* (Figure 5A). Figures 5B–D presented the measured values of intestinal villus height, crypt depth, and the ratio of villus height/crypt depth. Compared with the other three groups, the villus height of the duodenum, jejunum, and ileum in High group significantly decreased ($P < 0.05$), while the crypt depth dramatically increased ($P < 0.05$). Furthermore, we found that the villus height of both Low and Medium groups significantly decreased ($P < 0.05$). Compared to Control group, villus height/crypt depth decreased ($P < 0.05$) in High group. However, the villus height/crypt depth of jejunum in Low group had no difference with Control group.

Effect of *Clostridium perfringens* Treatment on Inflammatory Cytokines and Immunoglobulin of Mice

High and Medium dose *C. perfringens* infection significantly increased ($P < 0.05$) the concentration of IL-1 β , IL-6, and TNF- α compared with Control group (Figures 6A–C). However, the Low group had no difference ($P > 0.05$) compared with Control group. For IgA, IgG, and sIgA concentrations (Figures 6D–F), the results were opposite to pro-inflammatory factors. Compared to Control group, the High group did not show a difference ($P > 0.05$) in the concentrations of IgA, IgG, and sIgA, while the Medium and Low dose group showed a remarkable upward trend ($P < 0.05$).

TABLE 3 | The time of clinical symptoms and the number of deaths after gavage of different doses.

| Group | Number of bacteria inoculated (CFU/mL) | Time to onsets of symptoms (h) | Number of deaths |
|---------|--|--------------------------------|------------------|
| Control | 0 | N | 0 |
| Low | 8.0×10^7 | 96 | 1 |
| Medium | 4.0×10^8 | 48 | 3 |
| High | 2.0×10^9 | 24 | 4 |

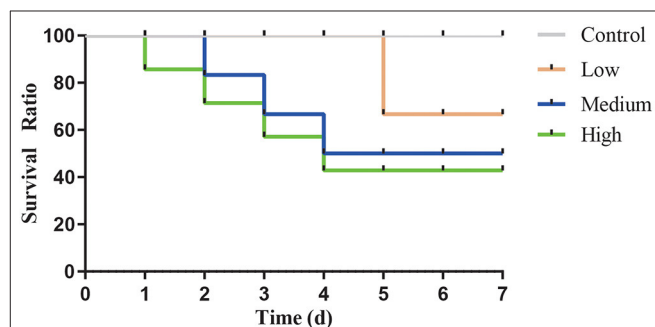


FIGURE 4 | The survival curve after intragastric administration of *Clostridium perfringens*.

Tight Junctions and Apoptosis Related Genes Expression

The tight junction-related genes (*ZO-1*, *Occludin*, *Claudin1*, and *MUC2*) in the jejunum down-regulated significantly ($P < 0.05$) in all *C. perfringens* infection groups compared to Control group (Figures 7A–D). Furthermore, with the dose rising, the gene expression of tight junctions decreased seriously. Pro-apoptosis genes including *Bax*, *p53*, *Caspase-3*, and *Caspase-9* elevated dramatically ($P < 0.05$) in the High group and Medium group in contrast to Control group and Low group (Figures 7E–H). High group enhanced the pro-apoptosis genes' expression stronger than other groups. Similarly, the anti-apoptosis gene (*Bcl-2*) saw a notable decrease ($P < 0.05$) among three *C. perfringens* stimulated groups compared with Control group (Figure 7I).

Ileal and Cecal *Clostridium perfringens* Enumeration

Figure 8 showed the results of the *C. perfringens*, *Escherichia coli*, and *Lactobacillus* enumeration in two different segments of small intestine in mice. Compared to Control group, the population of *C. perfringens* and *Escherichia coli* increased significantly in cecum and ileum ($P < 0.05$) by *C. perfringens* challenge. The genes copies of *C. perfringens* and *Escherichia coli* enriched remarkably ($P < 0.05$) in High group compared to Low and Medium group. Meanwhile, the population of *Lactobacillus* remained steady ($P > 0.05$) in ileum among four groups, while the *Lactobacillus* of cecal digesta decreased dramatically ($P < 0.05$) in High group in contrast to Control group.

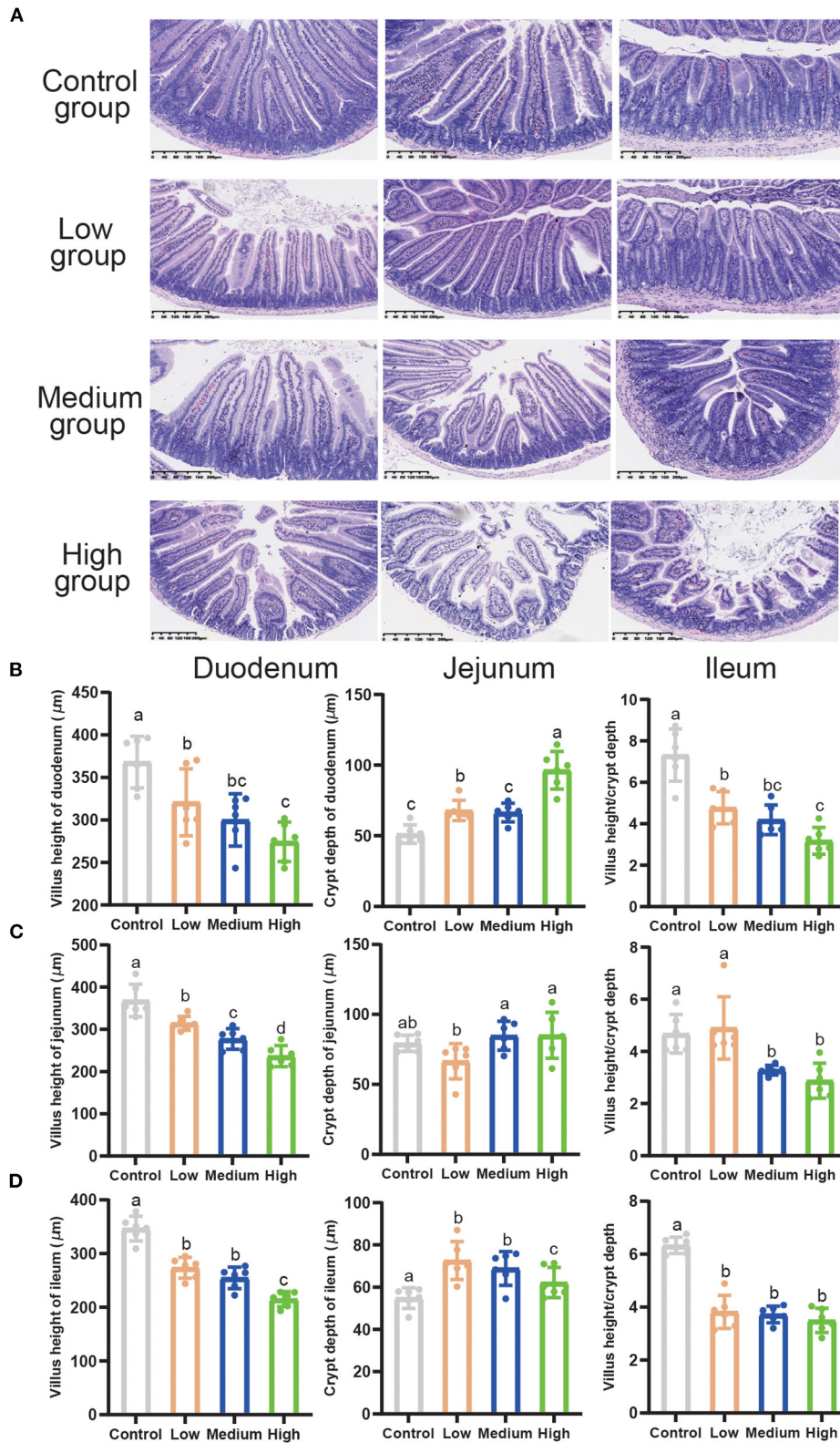
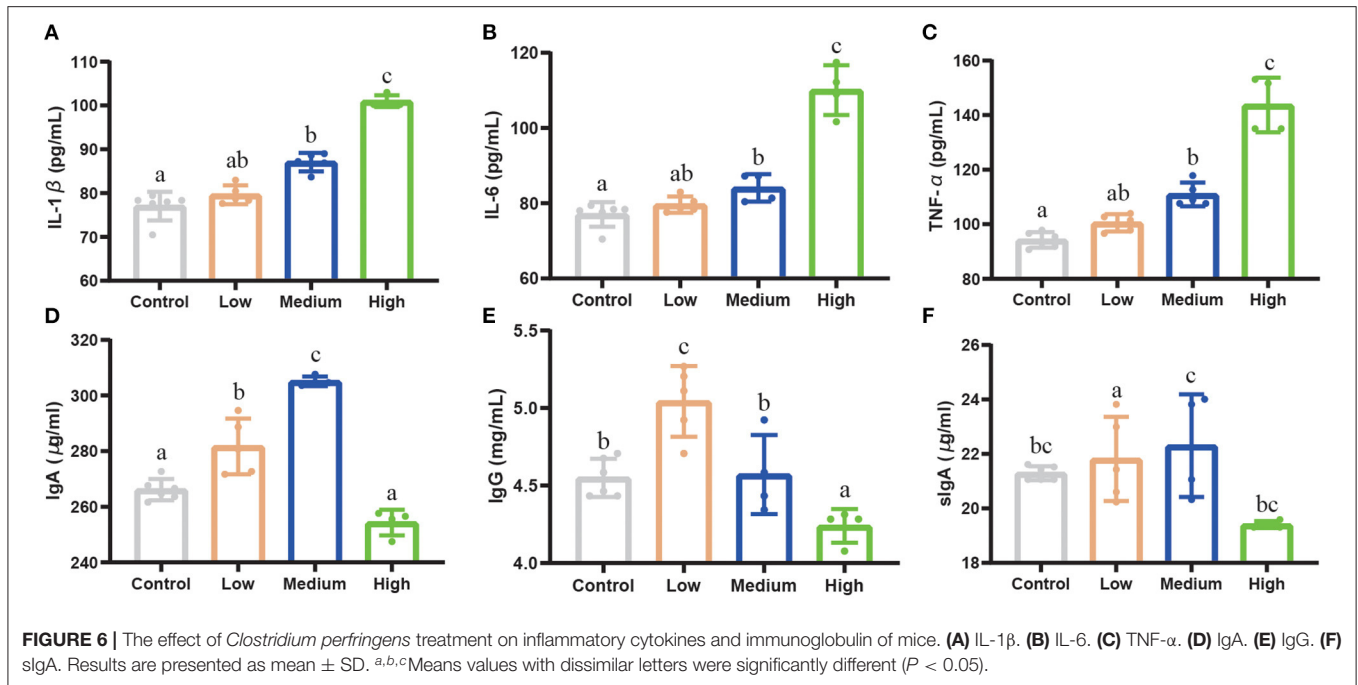


FIGURE 5 | The effects of *Clostridium perfringens* treatment on the intestines of mice. **(A)** Duodenum, jejunum, ileum, liver, and spleen were stained with hematoxylin and eosin (H&E) (bars = 330 µm). **(B)** Villus height of duodenum, crypt depth of duodenum, and villus height/crypt depth. **(C)** Villus height of jejunum, crypt depth of jejunum, and villus height/crypt depth. **(D)** Villus height of ileum, crypt depth of ileum, and villus height/crypt depth. All the values contained six repetitions. *a,b,c,d* Means values with dissimilar letters were significantly different ($P < 0.05$).



DISCUSSION

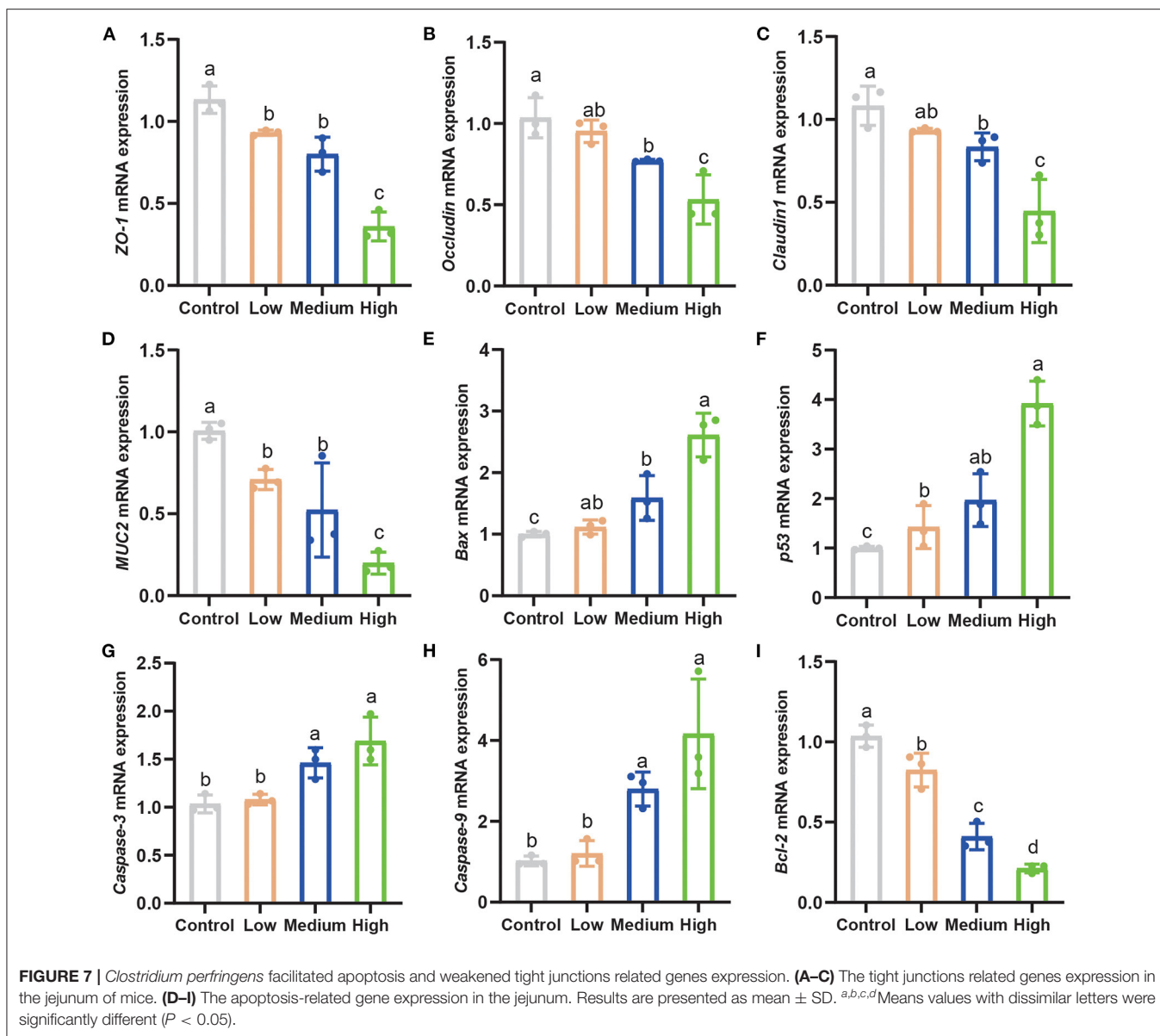
Enteric disease that occurs in suckling and finishing pigs is usually caused by *C. perfringens* type A or type C, and this pathogen has been linked to necrotizing enterocolitis and villous atrophy in pig's intestines. Lesions are always most severe in the small intestine, especially the jejunum and ileum (16). Isolating the pathogenic *C. perfringens* and establishing infection animal model is an essential step to prevent and treat clinical diseases in the animal production process. In this study, we aimed to investigate the suitable concentration of *C. perfringens* to establish a mouse model.

We used the same method as Kareem Rashid Rumah et al. to isolate the type B *P. aeruginosa* strain by sandwiching fecal samples in TSC agar (30). Similarly, Ruofan Wang et al. and Rodrigo et al. had successfully accessed the sequencing biotechnology to determine the genera of isolation bacteria from soil (*C. perfringens* type A) and cat (*C. perfringens* type A), respectively (31, 32).

For the animal experiment, the growth performance of three different concentrations of *C. perfringens* were different from Control group, which indicated that *C. perfringens* treatment can influence the growth status of mice. Furthermore, with the dose increasing, the daily feed intake and colon length decreased significantly ($P < 0.05$) compared with Control group. However, spleen index increased significantly ($P < 0.05$) in Medium and High group. The main reason for these results is the damage to the intestinal segments of the mice and a series of immune responses caused by *C. perfringens* infection, resulting in reduced food intake and swelling of the organs. The survival curve illustrated that the LD50 dose is High dose (2.0×10^9 CFU/mL).

For oral challenge mouse model studies, Mariano E. Fernandez-Miyakawa et al. used *C. perfringens* type D to study the lethality (7 of 10 type D isolates were lethal) and they provided the lethality of the seven type D isolates varying from 14 to 100% (15). Similarly, Uzal et al. (17) found that intragastric or intraduodenal challenge in mice can trigger respiratory distress and abdominal distension, and they found that, when inoculated into mice by intragastric gavage, 7 of 14 type C isolates were lethal, while when inoculated intraduodenally, all strains were lethal. These results indicated that pathogens have a different ability to produce toxins and LD50 were unequal even in the same type of *C. perfringens*. Our study indicated that this porcine *C. perfringens* type A isolated from our laboratory is infectious and toxic and it is suitable for building the mouse model.

It is known that the physical barrier is the first line of defense against pathogens invading into the intestine, and gut health level is related to villus atrophy and crypt hyperplasia degree (33). Our previous study indicated that *C. perfringens* infection can trigger serious villous atrophy and intestinal morphology disruption (21). This study also demonstrated that High dose *C. perfringens* inoculation impaired the development of the small intestinal morphology, weakened the villus morphology, decreased the ratio of villus height/crypt depth, and triggered an irreparable effect on the crypt depth in the small intestine. Some studies in broilers presented the same results in intestinal morphology (34–37). Other studies found that the *C. perfringens* enterotoxin (CPE), which is the main toxin produced by *C. perfringens* type A, displayed a dose-dependent effect and CPE can induce the intestinal injury (38–40). These studies focused on the toxæmic outcome of toxin absorption from the intestine into the circulation, and they did not adequately examine the specific changes that occur during *C. perfringens* infection. In the present



study, we used a mouse model by oral gavage to understand the pathogenesis of porcine gas-producing podoconiosis. Our results suggested that high doses of *C. perfringens* have a negative effect on intestinal damage and the High dose (2.0×10^9 CFU/mL) could construct the mouse model, too. One possible reason is that the high dose of *C. perfringens* causes an imbalance in the intestinal flora and *C. perfringens* can overgrow and induce inflammation in the intestine of mice, leading to a series of negative effects (weight loss, decreased expression of tight junction proteins, intestinal morphological damage, etc.).

To some extent, the serum inflammatory cytokines and immunoglobulin can reflect the physiological and immune status of mice after *C. perfringens* infection. Serum IL-1 β , IL-6, and TNF- α are indicators of pro-inflammatory reaction, which can be observed in the *C. perfringens* infected animals (41–43). IgA

can mediate a variety of protective functions and also has both anti-inflammatory and pro-inflammatory effects (44). Similar studies report that IgA deficiency can induce the inflammation, specifically in the ileum. IgG is the major serum immunoglobulin involved in mediating a protective inflammatory response (45). Secretory immunoglobulin A (sIgA) is the most abundant colonic antibody antigen and it can improve the immune status of animals (46). Following infection with opportunistic pathogens, cytokine expression of IL-1 β , IL-6, and TNF- α in the mucosa and serum increased significantly ($P < 0.05$), which resulted in decreased immunity (47, 48). Our results demonstrated that with the infectious dose increasing, the pro-inflammatory cytokines rose significantly ($P < 0.05$) compared with Control group, especially in High group. IgA, IgG, and fecal sIgA increased ($P < 0.05$) significantly in Low group and Medium group,

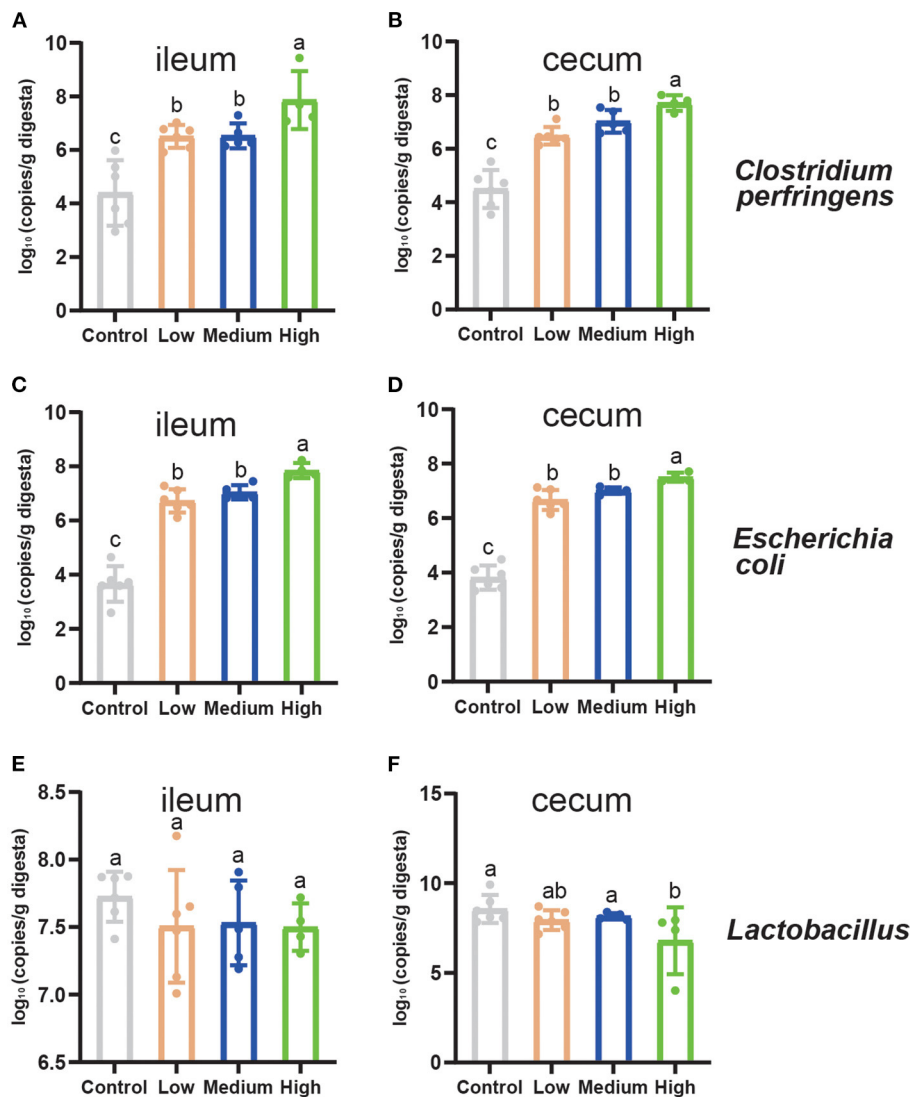


FIGURE 8 | The quantitation of intestinal microbiota of mice on d 8. **(A)** The population of *Clostridium perfringens* in the ileum. **(B)** The population of *Clostridium perfringens* in the cecum. **(C)** The population of *Escherichia coli* in the ileum. **(D)** The population of *Escherichia coli* in the cecum. **(E)** The population of *Lactobacillus* in the ileum. **(F)** The population of *Lactobacillus* in the cecum. Tight junctions related genes expression in the jejunum of mice. Results are presented as mean \pm SD (The data were presented as \log_{10} gene copies/g of intestinal digesta). ^{a,b,c}Means values with dissimilar letters were significantly different ($P < 0.05$).

which indicated that mild pathogens infection can stimulate the immunoglobulin secretion. However, the High dose may lower the immune status of an animal so that the host could not respond to pathogen invasion adequately and accurately.

Tight junctions play a vital role in separating tissue compartments and maintaining cellular polarity (49). The core complex is composed of ZO, Occludin, and Claudin family members, which connect the intestinal epithelial cells and regulate paracellular permeability (50). Meanwhile, the MUC2 is the structural component of the intestinal epithelium mucus layer and its expression is lowered in inflammatory bowel disease (51). Epithelial damage, in particular the tight junction proteins and mucins affecting the protective properties, likely induces

the inflammation (52). The tight junctions related genes and MUC2 gene expression (**Figures 7A–D**) in the jejunum of mice decreased significantly ($P < 0.05$) in Medium and High group. Our results demonstrated that the adequate concentrations of porcine *C. perfringens* can injure the tight junctions seriously in the jejunum of mice. Additionally, apoptosis is critical for the normal development and function of multicellular organisms, which are initially activated by the imbalance proteins expression, such as pro-apoptosis protein Bax and anti-apoptosis protein Bcl-2 (53). After the imbalance occurs, the apoptosis process began, and the main characteristic is the release of cytochrome c from the mitochondria. Then Caspase-9 and downstream executioner Caspases-3 are activated, thereby initiating cell apoptosis (54).

In addition, p53 protein can induce apoptosis by inhibiting the expression of anti-apoptosis gene (survivin) and promoting the pro-apoptosis (Bax), thereby triggering apoptosis through caspase-dependent pathway (55). Using a mouse model, *C. perfringens* enterotoxin was shown to cause intestinal caspase-3 activation in a dose- and time-dependent manner (38). Using the broiler model which was infected by *C. perfringens*, the pro-apoptosis related genes also showed a significant increase ($P < 0.05$) and a dramatic decrease ($P < 0.05$) in anti-apoptosis related genes (56). Our previous study presented the same results, C57B/L mice infected with *C. perfringens* ATCC 13124 showed a significant decrease in jejunal Bcl-2 gene expression and a significant increase in Bax, p53, Caspase-3 and Caspase-9 gene expression (21). In the present study, we found that the High group can induce a stronger apoptosis signal compared with other groups.

Many bacteria have been shown to coexist with *C. perfringens* when the infection occurs, including *Escherichia coli*. *Escherichia coli* is a major enteric pathogen causing intestinal diseases (57). Gao et al. exerted the same method and established the standard curve of *Escherichia coli* K88 to detect it in the small intestinal contents of piglets (58). Meanwhile, Zhui Li et al. used a similar method to detect the *C. perfringens* type A content in ileum and cecum of broilers (25). All these studies found that the aimed bacterial content in infection group increased significantly ($P < 0.05$) compared to control group. As with *C. perfringens* infection, the population of *Escherichia coli* increased significantly, which might influence the intestine to counteract the serum endotoxin secreted by *C. perfringens* (25). *Lactobacillus* species have been known as probiotics, which can produce bacteriostatic bacteriocin-like compound and acids, including lactic acid (59). Other studies reported that *Lactobacillus* can prevent the proliferation of pathogenic bacteria and regulate the intestinal flora (60, 61). In addition, *Lactobacillus* plays an important role in maintaining the gut health of animal (62) and modulating immunity (63). In the present study, *C. perfringens* challenge significantly increased ($P < 0.05$) the population of *C. perfringens* and *Escherichia coli* in the ileum and cecum, which are consistent with previous studies (24, 64). However, compared to Control group, the *Lactobacillus* of cecum significantly decreased ($P < 0.05$). Other previous studies (24, 64) reported that, after being challenged with *C. perfringens*, the *Lactobacillus* of cecum also increased, while our study showed the opposite. One possible reason to explain this is the high dose of *C. perfringens* could alter the balance of

microbial community in mice, while low and medium doses might alter the microbiota composition to some degree or not at all.

CONCLUSION

In summary, the present study evaluated the effects of different porcine *C. perfringens* dose (High: 2.0×10^9 CFU/mL, Medium: 4.0×10^8 CFU/mL, Low: 8.0×10^7 CFU/mL) treatments in mice by oral gavage. The High group meet the requirements for constructing mouse models by reducing growth performance, damaging intestinal morphology, reducing immune status, promoting apoptosis, and increasing the number of pathogens. Furthermore, these results provided an experimental and theoretical basis for the construction of porcine *C. perfringens* infection model in mice.

DATA AVAILABILITY STATEMENT

The datasets presented in this study can be found in online repositories. The names of the repository/repositories and accession number(s) can be found in the article/supplementary material.

ETHICS STATEMENT

The animal study was reviewed and approved by Institutional Animal Care and Use Committee at Zhejiang University.

AUTHOR CONTRIBUTIONS

ZJ: conceptualization, methodology, investigation, and writing original draft. WS, WL, CW, and SD: investigation and visualization. YZ and TG: formal analysis and visualization. XW: writing–review and editing. MJ, ZL, and YW: resources, writing–review, editing, and supervision. All authors contributed to the article and approved the submitted version.

FUNDING

The authors thank the specialized research fund from Major Science and Technology Projects of Zhejiang (2021C02008, 2022C02043, and CTZB-2020080127), China Agriculture Research System of MOF and MARA (CARS-35), National Center of Technology Innovation for Pigs.

REFERENCES

- Hassan KA, Elbourne LD, Tetu SG, Melville SB, Rood JI, Paulsen IT. Genomic analyses of *Clostridium perfringens* isolates from five toxinotypes. *Res Microbiol.* (2015) 166:255–63. doi: 10.1016/j.resmic.2014.10.003
- Uzal AF, Navarro AM, Li J, Freedman CJ, Shrestha A, McClane BA. Comparative pathogenesis of enteric clostridial infections in humans and animals. *Anaerobe.* (2018) 53:11–20. doi: 10.1016/j.anaerobe.2018.06.002
- Chahal K. Bacteria emerging as an opportunistic pathogen. *Int J Curr Sci Res Rev.* (2021) 4:401–7. doi: 10.47191/ijcsrr/V4-i5-12
- Kiu R, Hall LJ. An update on the human and animal enteric pathogen *Clostridium perfringens*. *Emerg Microbes Infect.* (2018) 7:141. doi: 10.1038/s41426-018-0144-8
- Marlow AM, Luna-Gierke ER, Griffin MP, Vieira AR. Foodborne disease outbreaks in correctional institutions-United States, 1998–2014. *Am J Public Health.* (2017) 107:1150–6. doi: 10.2105/AJPH.2017.303816
- Scallan E, Hoekstra MR, Mahon EB, Jones FT, Griffin PM. An assessment of the human health impact of seven leading foodborne pathogens in the United States using disability adjusted life years. *Epidemiol Infect.* (2015) 143:2795–804. doi: 10.1017/S0950268814003185

7. Timbermont L, Haesebrouck F, Ducatelle R, Van Immerseel F. Necrotic enteritis in broilers: an updated review on the pathogenesis. *Avian Pathol.* (2011) 40:341–7. doi: 10.1080/03079457.2011.590967
8. Mwangi S, Timmons J, Fitz-Coy S, Parveen S. Characterization of *Clostridium perfringens* recovered from broiler chicken affected by necrotic enteritis. *Poult Sci.* (2019) 98:128–35. doi: 10.3382/ps/pey332
9. Posthaus H, Kittl S, Tarek B, Bruggisser J. *Clostridium perfringens* type C necrotic enteritis in pigs: diagnosis, pathogenesis, and prevention. *J Vet Diagn Invest.* (2020) 32:203–12. doi: 10.1177/1040638719900180
10. Perlman RL. Mouse models of human disease: an evolutionary perspective. *Evol Med Public Health.* (2016) 2016:170–6. doi: 10.1093/emph/eow014
11. Awad, MM, Ellemor, MD, Boyd, LR, et al. Synergistic effects of alpha-toxin and perfringolysin O in *Clostridium perfringens*-mediated gas gangrene. *Infect Immun.* (2001) 69:7904–10. doi: 10.1128/IAI.69.12.7904-7910.2001
12. O'Brien, KD, Therit, HB, Woodman, EM, Melville SB. The role of neutrophils and monocytic cells in controlling the initiation of *Clostridium perfringens* gas gangrene. *FEMS Immunol Med Microbiol.* (2007) 50:86–93. doi: 10.1111/j.1574-695X.2007.00235.x
13. Schoster A, Kokotovic B, Permin A, Pedersen, DP, Dal Bello F, et al. In vitro inhibition of *Clostridium difficile* and *Clostridium perfringens* by commercial probiotic strains. *Anaerobe.* (2013) 20:36–41. doi: 10.1016/j.anaerobe.2013.02.006
14. Caserta, AJ, Robertson, LS, Saputo J, Shrestha A, et al. Development and application of a mouse intestinal loop model to study the *in vivo* action of *Clostridium perfringens* enterotoxin. *Infect Immun.* (2011) 79:3020–7. doi: 10.1128/IAI.01342-10
15. Fernandez-Miyakawa EM, Sayeed S, Fisher JD, Poon R, Adams V, Rood JJ, et al. Development and application of an oral challenge mouse model for studying *Clostridium perfringens* type D infection. *Infect Immun.* (2007) 75:4282–8. doi: 10.1128/IAI.00562-07
16. Uzal AF, McClane AB, Cheung KJ, Theoret J, Garcia PJ, Moore JR, et al. Animal models to study the pathogenesis of human and animal *Clostridium perfringens* infections. *Vet Microbiol.* (2015) 179:23–33. doi: 10.1016/j.vetmic.2015.02.013
17. Uzal AF, Saputo J, Sayeed S, Vidal EJ, Fisher JD, Poon R, et al. Development and application of new mouse models to study the pathogenesis of *Clostridium perfringens* type C Enterotoxemias. *Infect Immun.* (2009) 77:5291–9. doi: 10.1128/IAI.00825-09
18. Trajkovic S, Dobric S, Jacevic V, Dragojevic-Simic V, Milovanovic Z, Dordevic A. Tissue-protective effects of fullereneol C60(OH)24 and amifostine in irradiated rats. *Colloids Surf B Biointerfaces.* (2007) 58:39–43. doi: 10.1016/j.colsurfb.2007.01.005
19. Wen C, Guo Q, Wang W, Duan Y, Zhang L, Li J, et al. Taurine alleviates intestinal injury by mediating tight junction barriers in diquat-challenged piglet models. *Front Physiol.* (2020) 11:449. doi: 10.3389/fphys.2020.00449
20. Wen C, Li F, Guo Q, Zhang L, Duan Y, Wang W, et al. Protective effects of taurine against muscle damage induced by diquat in 35 days weaned piglets. *J Anim Sci Biotechnol.* (2020) 11:56. doi: 10.1186/s40104-020-00463-0
21. Jiang Z, Li W, Su W, Wen C, Gong T, Zhang Y, et al. Protective effects of *Bacillus amyloliquefaciens* 40 against *Clostridium perfringens* infection in mice. *Front Nutr.* (2021) 8:733591. doi: 10.3389/fnut.2021.733591
22. Wang Y, Liu F, Liu M, Zhou X, Wang M, Cao K, et al. Curcumin mitigates aflatoxin B1-induced liver injury via regulating the NLRP3 inflammasome and Nrf2 signaling pathway. *Food Chem Toxicol.* (2022) 161:112823. doi: 10.1016/j.fct.2022.112823
23. Yang H, Wang Y, Yu C, Jiao Y, Zhang R, Jin S, et al. Dietary resveratrol alleviates AFB1-induced ileum damage in ducks via the Nrf2 and NF-κB/NLRP3 signaling pathways and CYP1A1/2 expressions. *Agriculture.* (2022) 12:54. doi: 10.3390/agriculture12010054
24. Du E, Gan L, Li Z, Wang W, Liu D, Guo Y. *In vitro* antibacterial activity of thymol and carvacrol and their effects on broiler chickens challenged with *Clostridium perfringens*. *J Anim Sci Biotechnol.* (2015) 6:58. doi: 10.1186/s40104-015-0055-7
25. Li Z, Wang W, Liu D, Guo Y. Effects of *Lactobacillus acidophilus* on the growth performance and intestinal health of broilers challenged with *Clostridium perfringens*. *J Anim Sci Biotechnol.* (2018) 9:25. doi: 10.1186/s40104-018-0243-3
26. Wise, GM, Siragusa GR. Quantitative analysis of the intestinal bacterial community in one- to three-week-old commercially reared broiler chickens fed conventional or antibiotic-free vegetable-based diets. *J Appl Microbiol.* (2007) 102:1138–49. doi: 10.1111/j.1365-2672.2006.03153.x
27. Rinttila T, Kassinen A, Malinen E, Krogius L, Palva A. Development of an extensive set of 16S rDNA-targeted primers for quantification of pathogenic indigenous bacteria in faecal samples by real-time PCR. *J Appl Microbiol.* (2004) 97:1166–77. doi: 10.1111/j.1365-2672.2004.02409.x
28. Deplancke B, Vidal O, Ganessunker D, Donovan SM, Mackie RI, Gaskins HR. Selective growth of mucolytic bacteria including *Clostridium perfringens* in a neonatal piglet model of total parenteral nutrition. *Am J Clin Nutr.* (2002) 76:1117–25. doi: 10.1093/ajcn/76.5.1117
29. Lee C, Kim J, Shin, GS, Hwang S. Absolute and relative QPCR quantification of plasmid copy number in *Escherichia coli*. *J Biotechnol.* (2006) 123:273–80. doi: 10.1016/j.jbiotec.2005.11.014
30. Rumah, RK, Linden J, Fischetti, AV, Vartanian T. Isolation of *Clostridium perfringens* type B in an individual at first clinical presentation of multiple sclerosis provides clues for environmental triggers of the disease. *PLoS ONE.* (2013) 8:e76359. doi: 10.1371/journal.pone.0076359
31. Silva SRO, Ribeiro MG, de Paula, LC, Pires, HI, et al. Isolation of *Clostridium perfringens* and *Clostridioides difficile* in diarrheic and nondiarrheic cats. *Anaerobe.* (2020) 62:102164. doi: 10.1016/j.anaerobe.2020.102164
32. Wang R, Zong W, Qian C, Wei Y, Yu R, Zhou Z. Isolation of *Clostridium perfringens* strain W11 and optimization of its biohydrogen production by genetic modification. *Int J Hydrogen Energy.* (2011) 36:12159–67. doi: 10.1016/j.ijhydene.2011.06.105
33. Iftekhar A, Sigal M. Defence and adaptation mechanisms of the intestinal epithelium upon infection. *Int J Med Microbiol.* (2021) 311:151486. doi: 10.1016/j.ijmm.2021.151486
34. Caly, LD, D'Inca R, Auclair E, Drider D. Alternatives to antibiotics to prevent necrotic enteritis in broiler chickens: a microbiologist's perspective. *Front Microbiol.* (2015) 6:1336. doi: 10.3389/fmicb.2015.01336
35. Jayaraman S, Thangavel G, Kurian H, Mani R, Mukkalil R, Chirakkal H. *Bacillus subtilis* PB6 improves intestinal health of broiler chickens challenged with *Clostridium perfringens*-induced necrotic enteritis. *Poult Sci.* (2013) 92:370–4. doi: 10.3382/ps.2012-02528
36. Knap I, Lund B, Kehlet, BA, Hofacre C, Mathis G. *Bacillus licheniformis* prevents necrotic enteritis in broiler chickens. *Avian Dis.* (2010) 54:931–5. doi: 10.1637/9106-101509-ResNote.1
37. Zhao Y, Fu J, Li P, Chen N, Liu Y, Liu D, et al. Effects of dietary glucose oxidase on growth performance and intestinal health of AA broilers challenged by *Clostridium perfringens*. *Poult Sci.* (2021) 101:101553. doi: 10.1016/j.psj.2021.101553
38. Freedman, CJ, Navarro, AM, Morrell E, Beingesser J, et al. Evidence that *Clostridium perfringens* enterotoxin-induced intestinal damage and enterotoxemic death in mice can occur independently of intestinal caspase-3 activation. *Infect Immun.* (2018) 86:117. doi: 10.1128/IAI.00931-17
39. Fernandez-Miyakawa, EM, Jost, HB, Billington, JS, et al. Lethal effects of *Clostridium perfringens* epsilon toxin are potentiated by alpha and perfringolysin-O toxins in a mouse model. *Vet Microbiol.* (2008) 127:379–85. doi: 10.1016/j.vetmic.2007.09.013
40. Navarro MA, Shrestha A, Freedman JC, Beingesser B, McClane BA, Uzal FA. Potential therapeutic effects of mepacrine against *Clostridium perfringens* enterotoxin in a mouse model of enterotoxemia. *Infection Immunity.* (2019) 87:e00670–18. doi: 10.1128/IAI.00670-18
41. Mizoguchi A, Yano A, Himuro H, Ezaki Y, Sadanaga T, Mizoguchi E, et al. Clinical importance of IL-22 cascade in IBD. *J Gastroenterol.* (2018) 53:465–74. doi: 10.1007/s00535-017-1401-7
42. Zhou J, Xiong X, Yin J, Zou L, Wang K, Shao Y, et al. Dietary lysozyme alters sow's gut microbiota, serum immunity and milk metabolite profile. *Front Microbiol.* (2019) 10:177. doi: 10.3389/fmicb.2019.00177
43. Zhuo Y, Feng B, Xuan Y, Che L, Fang Z, Lin Y, et al. Inclusion of purified dietary fiber during gestation improved the reproductive performance of sows. *J Anim Sci Biotechnol.* (2020) 11:47. doi: 10.1186/s40104-020-00450-5
44. Olas K, Butterweck H, Teschner W, Schwarz, PH, Reipert B. Immunomodulatory properties of human serum immunoglobulin A: anti-inflammatory and pro-inflammatory activities in human monocytes

- and peripheral blood mononuclear cells. *Clin Exp Immunol.* (2005) 140:478–90. doi: 10.1111/j.1365-2249.2005.02779.x
45. Yoshikatsu Kaneko FN, Jeffrey Ravetch V. Anti-Inflammatory activity of immunoglobulin G resulting from Fc sialylation. *Science.* (2006) 313:1129597. doi: 10.1126/science.1129594
 46. Palm NW, de Zoete RM, Cullen WT, Barry AN, Stefanowski J, Hao L, et al. Immunoglobulin A coating identifies colitogenic bacteria in inflammatory bowel disease. *Cell.* (2014) 158:1000–10. doi: 10.1016/j.cell.2014.08.006
 47. Ewaschuk BJ, Murdoch KG, Johnson RI, Madsen LK, Field CJ. Glutamine supplementation improves intestinal barrier function in a weaned piglet model of *Escherichia coli* infection. *Br J Nutr.* (2011) 106:870–7. doi: 10.1017/S0007114511001152
 48. Nagaishi T, Watabe T, Kotake K, Kumazawa T, Aida T, Tanaka K, et al. Immunoglobulin A-specific deficiency induces spontaneous inflammation specifically in the ileum. *Gut.* (2021) 71:487–96. doi: 10.1136/gutjnl-2020-322873
 49. Willott E, Balda MS, Fanning AS, Jameson B, Van Itallie C, Anderson JM. The tight junction protein ZO-1 is homologous to the *Drosophila* discs-large tumor suppressor protein of septate junctions. *Proc Natl Acad Sci USA.* (1993) 90:7834–8. doi: 10.1073/pnas.90.16.7834
 50. König J, Wells J, Cani DP, García-Ródenas LC, MacDonald T, Mercenier A, et al. Human intestinal barrier function in health and disease. *Clin Transl Gastroenterol.* (2016) 7:54. doi: 10.1038/ctg.2016.54
 51. Kristien MAJ, Büller HA, OpdamFJM, Kim YS, Einerhand AWC, Dekker J. Biosynthesis of human colonic mucin: Muc2 is the prominent secretory mucin. *Gastroenterology.* (1994) 107:1352–63. doi: 10.1016/0016-5085(94)90537-1
 52. Van der Sluis M, De Koning AB, De Bruijn CA, Velcich A, Meijerink PJ, Van Goudoever BJ, et al. Muc2-deficient mice spontaneously develop colitis, indicating that MUC2 is critical for colonic protection. *Gastroenterology.* (2006) 131:117–29. doi: 10.1053/j.gastro.2006.04.020
 53. Strasser A, O'Connor L, Dixit VM. Apoptosis signaling. *Ann Rev Biochem.* (2000) 69:217–45. doi: 10.1146/annurev.biochem.69.1.217
 54. Cohen GM. Caspases: the executioners of apoptosis. *Biochem J.* (1997) 326:1–16. doi: 10.1042/bj3260001
 55. Reed JC. Mechanisms of apoptosis. *Am J Pathol.* (2000) 157:1415–30. doi: 10.1016/S0002-9440(10)64779-7
 56. Gong L, Wang B, Zhou Y, Tang L, Zeng Z, Zhang H, et al. Protective effects of *Lactobacillus plantarum* 16 and *Paenibacillus polymyxa* 10 against *Clostridium perfringens* infection in broilers. *Front Immunol.* (2021) 11:628374. doi: 10.3389/fimmu.2020.628374
 57. Kaper, BJ, Nataro, PJ, Mobley HL. Pathogenic *Escherichia coli*. *Nat Rev Microbiol.* (2004) 2:123–40. doi: 10.1038/nrmicro818
 58. Gao Y, Han F, Huang X, Rong Y, Yi H, Wang Y. Changes in gut microbial populations, intestinal morphology, expression of tight junction proteins, and cytokine production between two pig breeds after challenge with *Escherichia coli* K88: a comparative study. *J Anim Sci.* (2013) 91:5614–25. doi: 10.2527/jas.2013-6528
 59. Chateau N, Castellanos I, Deschamps AM. Distribution of pathogen inhibition in the *Lactobacillus* isolates of a commercial probiotic consortium. *J Appl Bacteriol.* (1993) 74:36–40. doi: 10.1111/j.1365-2672.1993.tb02993.x
 60. Frece J, Kos B, Svetec KI, Zgaga Z, Beganović J, Leboš A, et al. Synbiotic effect of *Lactobacillus helveticus* M92 and prebiotics on the intestinal microflora and immune system of mice. *J Dairy Res.* (2009) 76:98–104. doi: 10.1017/S0022029908003737
 61. Liu H, Zhang J, Zhang S, Yang F, Thacker, AP. Oral administration of *Lactobacillus fermentum* I5007 favors intestinal development and alters the intestinal microbiota in formula-fed piglets. *J Agric Food Chem.* (2014) 62:860–866. doi: 10.1021/jf403288r
 62. Tsai CC, Hsieh YH, Chiu HH, Lai YY, Liu HJ, Yu B, et al. Antagonistic activity against *Salmonella* infection *in vitro* and *in vivo* for two *Lactobacillus* strains from swine and poultry. *Int J Food Microbiol.* (2005) 102:185–94. doi: 10.1016/j.ijfoodmicro.2004.12.014
 63. Lin HW, Yu B, Lin KC, Hwang ZW, Tsen HY. Immune effect of heat-killed multistrain of *Lactobacillus acidophilus* against *Salmonella typhimurium* invasion to mice. *J Appl Microbiol.* (2007) 102:22–31. doi: 10.1111/j.1365-2672.2006.03073.x
 64. Sun Q, Liu D, Guo S, Chen Y, Guo Y. Effects of dietary essential oil and enzyme supplementation on growth performance and gut health of broilers challenged by *Clostridium perfringens*. *Animal Feed Sci Technol.* (2015) 207:234–44. doi: 10.1016/j.anifeedsci.2015.06.021

Conflict of Interest: The authors declare that the research was conducted in the absence of any commercial or financial relationships that could be construed as a potential conflict of interest.

Publisher's Note: All claims expressed in this article are solely those of the authors and do not necessarily represent those of their affiliated organizations, or those of the publisher, the editors and the reviewers. Any product that may be evaluated in this article, or claim that may be made by its manufacturer, is not guaranteed or endorsed by the publisher.

Copyright © 2022 Jiang, Su, Wen, Li, Zhang, Gong, Du, Wang, Lu, Jin and Wang. This is an open-access article distributed under the terms of the Creative Commons Attribution License (CC BY). The use, distribution or reproduction in other forums is permitted, provided the original author(s) and the copyright owner(s) are credited and that the original publication in this journal is cited, in accordance with accepted academic practice. No use, distribution or reproduction is permitted which does not comply with these terms.